Short communication

Characterization of $ZnFe_2O_4$ Nanoparticles Obtained by the Thermal Decomposition of $ZnFe_2(cin)_3(N_2H_4)_3$

Kalpanadevi Kalimuthu, Sinduja C. Rangasamy and Manimekalai Rakkiyasamy*

Department of Chemistry, Kongunadu Arts and Science College, Coimbatore, Tamilnadu, India

* *Corresponding author: E-mail: manimekalair@ymail.com*

Received: 06-09-2013

Abstract

$ZnFe_2O_4$ nanoparticles have been obtained from the inorganic precursor $ZnFe_2(cin)_3(N_2H_4)_3$ via thermal decomposition route. The precursor prepared by a simple precipitation method, was characterised by hydrazine and metal analyses, infrared spectral analysis and thermo gravimetric analysis. Using appropriate annealing conditions, $ZnFe_2O_4$ nanoparticles of average size around 9 nm were synthesised by the thermal treatment of the precursor. The nanoparticles were characterised for their size and structure using X-Ray Diffraction (XRD), High Resolution Transmission Electron Microscopic (HRTEM), Selected Area Electron Diffraction (SAED) and Scanning Electron Microscopic (SEM) techniques.

Keywords: $ZnFe_2O_4$ nanoparticles, XRD, HRTEM, SAED, SEM

1. Introduction

Nano-sized spinel ferrites have been extensively investigated in the recent past for their valuable electrical and magnetic properties, and applications in several important technological fields such as ferrofluids,[1] electronic gadgets, information storage, magnetic resonance imaging (MRI), drug-delivery technology and catalysis.[2] Zinc ferrite ($ZnFe_2O_4$), an important spinel ferrite, is a commercially important material and has been widely used as magnetic materials,[3] gas sensor,[4] catalysts,[5] photocatalysts,[6] absorbent materials,[7] magneto caloric pumps,[8] etc.

Various methods have been developed to synthesize nanocrystalline $ZnFe_2O_4$ such as mechanical alloying,[9] pulsed wire discharge,[10] sol-gel method,[11] microemulsion,[12] thermal transformation process,[13] hydrothermal methods,[14] etc. Among these established methods, thermal treatment has attracted immense interest owing to its simple process, cost-effectiveness and crystallization as well as the control of the morphologies, sizes and phase transformation. In the present study, we report the synthesis of nanocrystalline $ZnFe_2O_4$ by a simple thermal decomposition method at a relatively low cost and low time.

2. Experimental

2. 1. Preparation of Zinc Ferrous Cinnamate Hydrazinate $ZnFe_2(cin)_3(N_2H_4)_3$

This was prepared by the addition of an aqueous solution (50 mL) of hydrazine hydrate (1 mL, 0.02 mol) and cinnamic acid (1.18 g, 0.0079 mol) to the corresponding aqueous solution (50 mL) of zinc nitrate hexahydrate (0.058 g, 0.0019 mol) and ferrous sulphate hepta-hydrate (2.22 g, 0.0079 mol). The brown orange product formed immediately was kept aside for an hour for digestion, then filtered and washed with water, alcohol followed by diethylether and air dried.

2. 2. Preparation of Zinc Ferrite Nanoparticles

Zinc ferrite nanoparticles were obtained from the autocatalytic decomposition of the precursor. In this method, the dried precursor was transferred to a silica crucible and heated to red hot condition in an ordinary atmosphere for about 45 minutes. The precursor started decomposing violently. The total decomposition of $ZnFe_2(cin)_3(N_2H_4)_3$ led to the formation of $ZnFe_2O_4$, which are quenched to room temperature, ground well and stored.

3. Results and Discussion:

3. 1. Chemical Formula Determination of the Precursor

The hydrazine content in the precursor was determined by titration using KIO_3 as the titrant, by volumetric analysis under Andrew's condition.[15] The percentage of zinc and iron in the precursor was estimated by gravimetry as given in the Vogel's textbook,[15] which was then confirmed by EDX analysis. Of the total composition of the precursor, the percentage remaining belongs to cinnamate, which was then confirmed by elemental analysis. Based on the observed percentage of hydrazine (13.38), zinc (26.84) and iron (45.99) which are found to match closely with the calculated values (13.52), (26.97) and (46.62) for hydrazine, zinc and iron respectively, the chemical formula $ZnFe_2(cin)_3(N_2H_4)_3$ has been tentatively assigned to the precursor, zinc ferrous cinnamate hydrazinate.

3. 2. FT-IR Analysis of the Precursor

The infrared spectrum of the solid precursor sample was recorded by the KBr disc technique using a Shimadzu spectrophotometer. From the IR spectrum of $ZnFe_2(cin)_3(N_2H_4)_3$, it is observed that the N-N stretching frequency is seen at 975 cm^{-1}, which unambiguously proves the bidentate bridging nature of the hydrazine ligand.[16] The asymmetric and symmetric stretching frequencies of the carboxylate ions are seen at 1639 and 1411 cm^{-1}, respectively with the $\Delta\upsilon$ (υ_{asymm}-υ_{sym}) separation of 228 cm^{-1}, which indicate the monodentate linkage of the carboxylate groups. The N-H stretching is observed at 3371 cm^{-1}. The IR data thus confirms the formation of zinc ferrous cinnamate hydrazinate.

3. 3. Thermal Analysis of the Precursor

The simultaneous TGA-DSC study was carried out in Universal V4.5A TA Instrument in a nitrogen atmosphere from room temperature to 700 °C. As can be observed from Figure 1, the precursor loses weight in two particular steps. The first step is the dehydrazination of the two hydrazine molecules between room temperature and 175 °C with a weight loss of 9%. The corresponding peak in DSC is observed as an exotherm. The major weight loss of 60% on the TG curve from 175 to 430 °C is attributed to the second step involving the dehydrazination of the remaining one hydrazine molecule and decarboxylation of the precursor, which gives $ZnFe_2O_4$ as the final residue.

3. 4. Characterization of $ZnFe_2O_4$ Nanoparticles

3. 4. 1. XRD Analysis

XRD pattern of $ZnFe_2O_4$ nanoparticles recorded using an X-ray diffractometer (X'per PRO model) using Cu-Ka radiation, at 40 keV in the 2h range of 10–80 is shown in Figure 2. Six characteristic peaks can be indexed as the cubic structure $ZnFe_2O_4$, which is accorded with the reported data (JCPDS File No 73–1963). The peaks with 2θ values of 30.416, 35.609, 43.600, 53.500, 56.860, 62.759 correspond to the crystal planes (220), (311), (400), (422), (511), (440) of crystalline $ZnFe_2O_4$ respectively, with lattice constant a = 0.835 nm. The average crystallite size was calculated using Debye-Scherrer formula, $D = K\lambda/\beta\cos\theta$, where, θ is Bragg diffraction angle, K is Blank's constant, λ is the source wavelength (1.54), and β is the width of the XRD peak at half maximum height. The calculated average crystallite size of the $ZnFe_2O_4$ was found to be around 9

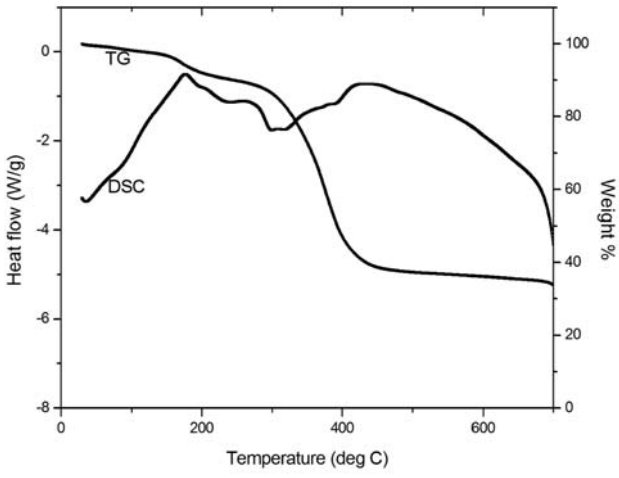

Fig.1. TG-DSC curve of $ZnFe_2(cin)_3(N_2H_4)_3$

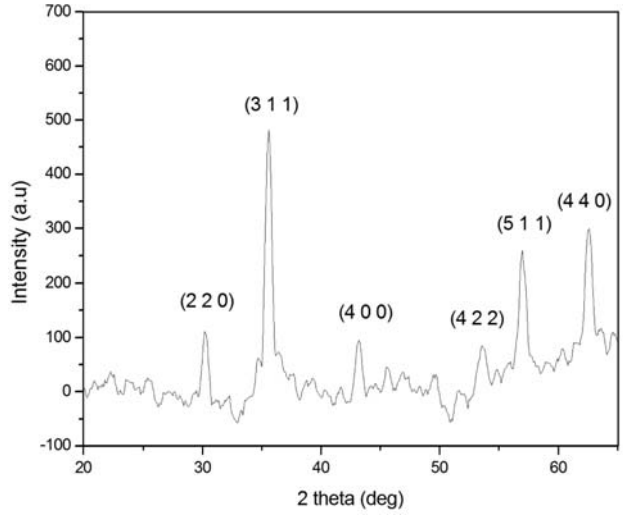

Fig. 2. XRD pattern of $ZnFe_2O_4$ nanoparticles

nm. No characteristic peaks for other impurities were detected, confirming that the product obtained is phase pure.

3. 4. 2. HRTEM Analysis

The HRTEM technique is used to visualize the shape and size of the $ZnFe_2O_4$ nanoparticles, formed in different sizes, ranging from polydispersed small spherical to large spherical shapes. HRTEM micrographs of $ZnFe_2O_4$, recorded on Jeol Jem 2100 advanced analytical electron microscope, which are shown in Figures 3a and 3b. The presence of some bigger particles should be attributed to be the aggregation or overlapping of some small particles. The average grain size observed from the micrograph is about 9 nm, which is in agreement with the calculation using Scherrer's equation. Figure 4 shows the selected area electron diffraction (SAED) pattern indicating sharp rings, which reveal the polycrystalline nature of the nanoparticles.

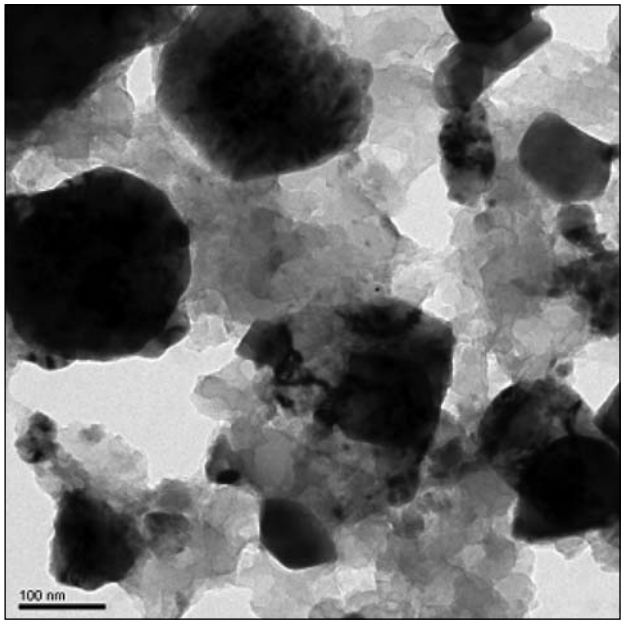

Fig. 3a. HRTEM image of $ZnFe_2O_4$ nanoparticles

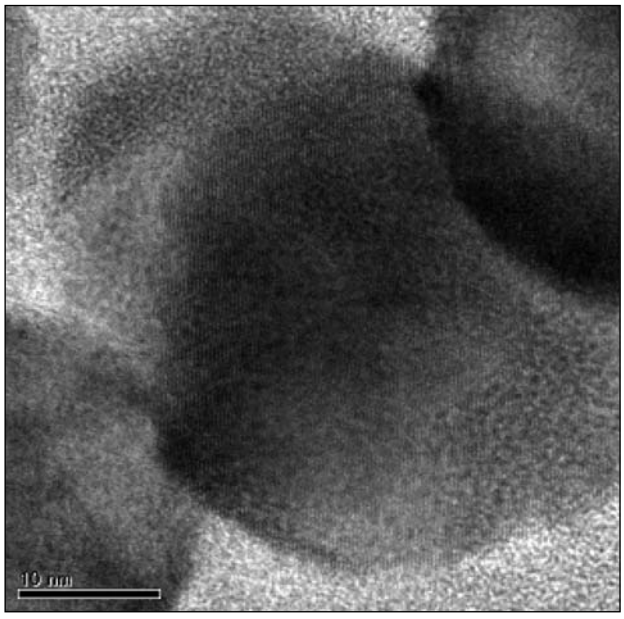

Fig. 3b. HRTEM image of $ZnFe_2O_4$ nanoparticles

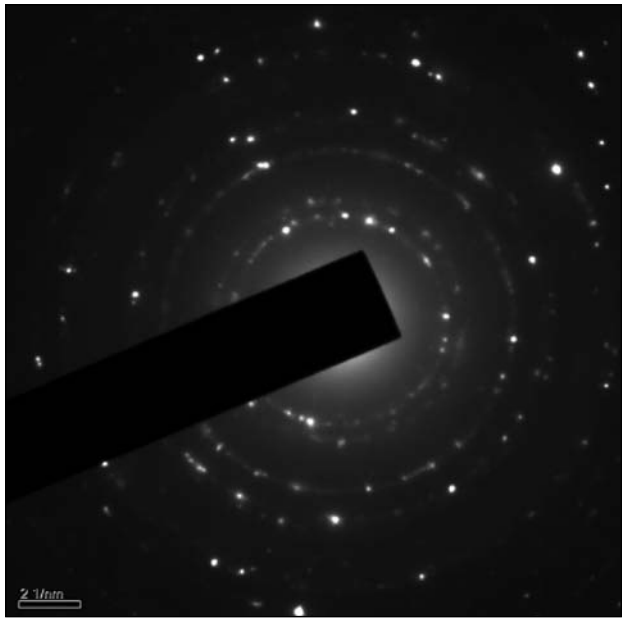

Fig.4. SAED pattern of $ZnFe_2O_4$ nanoparticles

3. 4. 3. SEM Analysis

The morphology of $ZnFe_2O_4$ was characterised by scanning electron microscope performed with a HITACHI Model S-3000H. The SEM pictures in Figures 5 a and 5 b clearly show randomly distributed grains with very smaller size and agglomeration of particles.

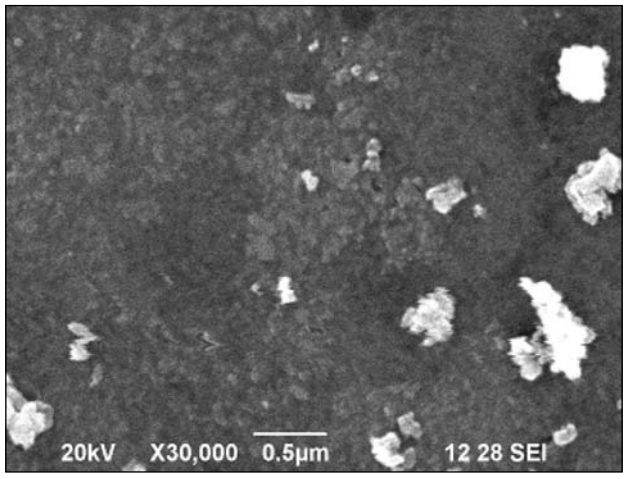

Fig. 5a. SEM image of $ZnFe_2O_4$ nanoparticles

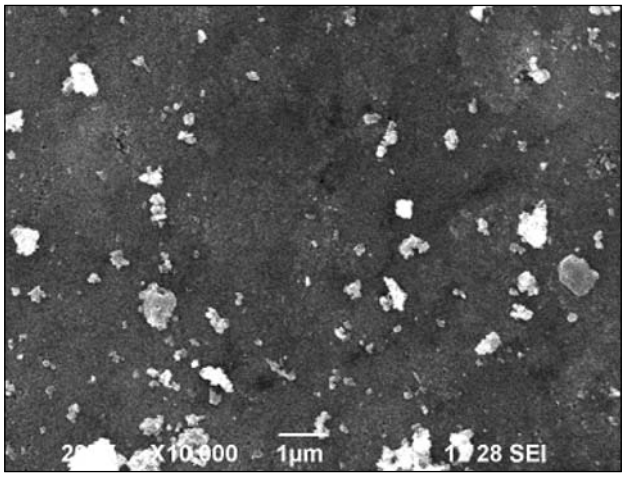

Fig. 5b. SEM image of $ZnFe_2O_4$ nanoparticles

The composition of the sample is given in table 1. EDX spectrum of $ZnFe_2O_4$ nanoparticles is presented in Figure 6, which furnishes the chemical compositional analysis of the nanoscale $ZnFe_2O_4$.

Compound	Zinc (%)		Iron (%)	
	Obs.	Calc.	Obs.	Calc.
$ZnFe_2O_4$	26.84	26.97	45.00	46.32

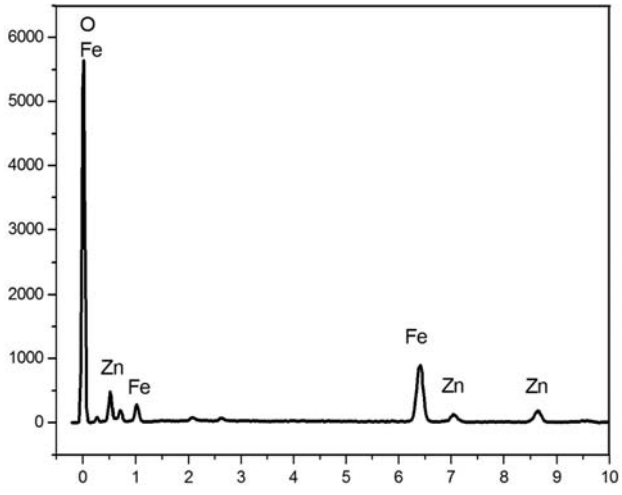

Fig. 6. EDX spectrum of $ZnFe_2O_4$ nanoparticles

4. Conclusion

$ZnFe_2O_4$ nanoparticles were effectively synthesised through a simple and novel thermal decomposition method from the corresponding inorganic precursor, $ZnFe_2(cin)_3(N_2H_4)_3$ and characterised by XRD, TEM, SAED and SEM techniques. The average particle size of $ZnFe_2O_4$ nanoparticles determined from XRD and TEM is about 9 nm. The present method is uncomplicated and commercially viable. It is also efficient in terms of time and equipment. Hence this method is a potential and facile route for the large scale industrial production of $ZnFe_2O_4$ nanoparticles.

5. References

1. J. Sun, Sh. Zhou, P. Hou, Y. Yang, J. Weng, X. Li, M. Li, *J. Biomedica. Mat. Res. A,* **2007**, *83*, 333–341.
2. L. J. Ma, L. S. Chen, S. Y. Chen, *J Phys Chem Solids*, **2007**, *68*, 1330–1335.
3. H. Deng, X. Li, Q. Peng, X. Wang, J. Chen, Y. Li, *Angew. Chem., Int. Ed. Engl.,* **2005**, *44*, 2782–2785.
4. X. Niu, W. Du, W. Du, *Sens. Actuators, B,* Chem., **2004**, *99*, 405–409.
5. J. A. Toledo-Antonio, N. Nava, M. Martínez, X. Bokhimi, *Appl. Catal., A Gen.,* **2002**, *234*, 137–144.
6. J. Qiu, C. Wang, M. Gu, *Mater. Sci. Eng., B, Solid-State Mater. Adv. Technol.,* **2004**, *112*, 1–4.
7. F. Tomás-Alonso, J. M. Palacios Latasa, *Fuel Process. Technol.,* **2004**, *86*, 191–203.
8. L. J. Love, J. F. Jansen, T. E. McKnight, Y. Roh, T. J. Phelps, L. W. Yeary, G. T. Cunningham, *T. IEEE, Mechatronics,* **2005**, *10*, 68–76.
9. Y. Shi, J. Ding, S. L. H. Tan, Z. Hu, *J Magn Magn Mater,* **2003**, *256*, 13–19.
10. Y. Kinemuchi, K. Ishizaka, H. Suematsu, W. Jiang, K. Yatsui, *Thin Solid Films,* **2002**, *407*, 109–113.
11. D. H. Chen, X. R. He, *Mater Res Bull.* **2001**, *36*, 1369–1377.
12. C. Liu, B. Zou, A. J. Rondinone, Z. J. Zhang, *J Phys Chem.,* **2000**, *B104*, 1141–1145.
13. H. M. Fan, J. B. Yi, Y. Yang, K. W. Kho, H. R. Tan, Z. X. Shen, et al., *ACS Nano,* **2009**, *3*, 2798–2808.
14. H. Li, H. Z. Wu, G. X. Xiao, *Powder Technol.,* **2010**, *198*, 157–166.
15. I. Vogel, "A Textbook of Quantitative Inorganic Analysis", 4th Ed., (Longman, UK, **1985**).
16. A. Braibanti, F. Dallavalle, M. A. Pellinghelli, E. Leporati, *Inorg. Chem.* **1968**, *7*, 1430–1433.

Povzetek

Nanodelce $ZnFe_2O_4$ smo pripravili s termičnim razpadom prekurzorja $ZnFe_2(cin)_3(N_2H_4)_3$. Prekurzor smo sintetizirali z metodo obarjanja, mu določili vsebnosti hidrazina in kovine ter ga karakterizirali z infraredčo spektroskopijo in termogravimetrično analizo. Z izbiro primernih pogojev termičnega razpade smo pripravili nanodelce $ZnFe_2O_4$ s povprečno velikostjo 9 nm, ki smo jih nadalje karakterizirali z različnimi tehnikami: rentgensko praškovno difrakcijo (XRD), z visokoločljivostnim transmisijskim elektronskim mikroskopom (HRTEM), elektronsko difrakcijo (SEAD) in z vrstičnim elektronskim mikroskopom (SEM).